2006

Optical imaging of radiolabeled drugs in tissue sections using the microImager

Paul Dungel
University of South Florida

Optical Imaging of Radiolabeled Drugs in Tissue Sections Using the MicroImager

by

Paul Dungel

A thesis submitted in partial fulfillment
of the requirements for the degree of
Master of Science in Biomedical Engineering
Department of Chemical Engineering
College of Engineering
University of South Florida

Major Professor: Yvonne Moussy, Ph.D.
Francis Moussy, Ph.D.
Mark Jaroszeski, Ph.D.

Date of Approval:
November 1, 2006

Keywords: autoradiography, dexamethasone, diffusion, subcutaneous tissue, tritium

Acknowledgments

I would like to thank and acknowledge Yvonne Moussy, Ph.D. for her encouragement and dedication to this project. I would also like to thank Lawrence Hersh, Ph.D. for his assistance in the mathematical modeling involved in this research. Finally, I would like to thank my colleagues in the Biosensors and Biomaterials Laboratory and all others around the university for their support over the past two years.

Table of Contents

List of Tables iii

List of Figures iv

Abstract vi

Chapter One MicroImager 1
Background of Radioimaging 1
Radiation 2
Emulsion Film Autoradiography 2
Phosphor Imaging 2
MicroImager Information 3
Operating Principles 3
Hardware Components of MicroImager 5
Scintillating Sheet 5
Image Intensifier Tube 5
CCD Camera 6
Software Components of MicroImager 6
Grid ROI 8
Circle ROI 8
Line Profile 9
Tracing 9
Previous Applications 10
Our Applications 11

Chapter Two Distribution of [^{3}H]Dexamethasone in Rat Subcutaneous Tissue after Delivery from Osmotic Pumps 12
Introduction 12
Materials and Methods 13
Materials 13
Preparation of Osmotic Pumps 14
Subcutaneous Implantation 14
Autoradiographic Imaging and Analysis 15
Mathematical Model 16
Results 20
Discussion 24

Chapter Three Diffusion of [^{3}H]Dexamethasone in Rat Subcutaneous Slices after Injection Measured by Digital Autoradiography 29
Introduction 29
Materials and Methods 29
Materials 29
Subcutaneous Injection 30
Autoradiographic Imaging and Analysis 30
Mathematical Model 31
Results 34
Discussion 36

Chapter Four Summary and Future Work 41
MicroImager 41
Osmotic Pump 41
Injection Study 42
Possible Future Work 42

References 43

List of Tables

Table 1.	Estimated D and k	21
Table 2.	Penetration distance of radioactivity from the tip of the catheter	23
Table 3.	Diffusion coefficients for dexamethasone in various media	25
Table 4.	Elimination constants of various agents in subcutaneous tissue	26
Table 5.	Estimated diffusion coefficient	36

List of Figures

Figure 1.	MicroImager with associated PC	3
Figure 2.	Scintillating sheet on slide	5
Figure 3.	The original autoradiogram of [^{3}H]dexamethasone as acquired by the MicroImager (left) and the same image with a psuedocolor LUT applied (right)	7
Figure 4.	Grid overlay on autoradiogram	8
Figure 5.	Circle ROI overlay on autoradiogram	8
Figure 6.	Line Profile on autoradiogram	9
Figure 7.	An optical image of rat subcutaneous tissue (left) and the [^{3}H]dexamethasone autoradiogram (right) with a manual trace of the optical image	10
Figure 8.	Concentration versus distance profiles obtained by solving the transient diffusion and elimination equation (eq 3) for various times until steady state is reached are shown	18
Figure 9.	Autoradiographic image from rat subcutaneous tissue obtained using the MicroImager after implantation of an osmotic pump containing [^{3}H]dexamethasone for 6 hrs	20
Figure 10.	Typical concentration profiles in the vicinity of the catheter tip at (a) 6 hr, (b) 24 hr and (c) 60 hr after implantation	22
Figure 11.	A typical H&E steaned tissue section from our study	27
Figure 12.	Concentration profiles for diffusion when a concentrated bolus of solute is deposited within a small region	33
Figure 13.	Image a shows a typical autoradiographic image obtained using the MicroImager 157 s after injection of [^{3}H]dexamethasone	35

Figure 14. Typical number of events versus distance profiles obtained using the MicroImager at (a) 157 s and (b) 20 min after implantation 35

Figure 15. Concentration profiles at the tail-end at (a) 157 s and (b) 20 min after injection. Data from only one angle per time period is shown 38

Optical Imaging of Radiolabeled Drugs in Tissue Sections Using the MicroImager

Paul Dungel

ABSTRACT

The MicroImager is a fast, high resolution, real time, digital autoradiographic imaging tool with broad applications. This study utilizes the MicroImager to evaluate radiolabeled drug behavior in subcutaneous tissue. Experiments were conducted in conjunction with mathematical models to determine the diffusion coefficient (D) and elimination constant (k) for radiolabeled dexamethasone.

Osmotic pumps containing [^{3}H]dexamethasone were implanted into rat subcutaneous tissue over 6h, 24 h, and 60 h. Local tissue was explanted and slides were prepared for imaging. The MicroImager was then used to quantify the local concentration of ^{3}H-dexamethasone in the tissue surrounding the tip of the osmotic pump. Betavision+ software was used to obtain local concentration profiles. These were then compared to a mathematical model to determine the diffusion coefficient and elimination constant for the radiolabeled drug. The diffusion coefficient for dexamethasone in rat subcutaneous tissue is $4.11 \pm 1.77 \times 10^{-10}$ m^2/s. The elimination constant is $3.65 \pm 2.24 \times 10^{-5}$ s^{-1}.

A similar experiment was conducted to determine the diffusion coefficient through different means. [^{3}H]dexamethasone was injected into the rat subcutaneous

tissue for a 2.5 min and a 20 min period. A different mathematical model was applied and the diffusion coefficient was found to be $4.01 \pm 2.01 \times 10^{-10}$ m^2/s.

Chapter One

MicroImager

Background of Radioimaging

The use of radioactive isotopes to investigate biological phenomenon is important for several reasons. Radioactive tracers are incorporated into the substance being studied and rarely inhibit the molecules motion or binding characteristics. Also, degradation of the signal does not decrease over time when using an appropriate isotope. This provides for long term storage and analysis without loss of data. This valuable tool in contemporary medicine had its beginnings over 80 years ago. Autoradiography was first applied to systemic biological investigation in 1924 by Lacassagne (1). Using photographic emulsions, Lacassagne studied Polonium distribution in tissues. Photographic emulsions have been used to evaluate the presence and location of radiation in tissues ever since.

Radiation

Elements (Hydrogen, Carbon, Iodine, etc) can exist naturally as unstable isotopes of stable atoms. They can regain their stability by emitting energy in the form of radiation. This radiation can have different forms and different energies. Alpha, gamma, and beta radiation have different characteristics and are associated with specific decay activities (2).

Alpha decay occurs when an alpha particle is emitted from the nucleus of an atom. An alpha particle is defined as ${}^{4}_{2}\mathrm{He}$. Gamma radiation has no mass and is capable of the greatest penetrative distance. This type of radiation is commonly used in X-ray imaging.

Beta radiation can have two forms. A β- particle is an electron while a β+ particle is a positron. Each of these has a mass 1/1840 that of a proton. If a β- particle is emitted from the nucleus, the transformation that occurs is that a neutron changes to an electron and a proton. On the other hand, if a β+ particle is emitted, a proton splits into a positron and a neutron. The type of decay that occurs is dependant on the specific element (2). Tritium, the radiolabel used in my experiments, emits β- particles that are then detected and analyzed.

Emulsion Film Autoradiography

The traditional method for visualizing radiation has been photographic emulsions. A photographic emulsion incorporates Silver Bromide (AgBr) crystals in a gelatin suspension. Upon exposure of the emulsion to a radioactive sample, areas of the crystal that are irradiated undergo a transformation. The free electron (β- particle) oxidized the silver and creates metallic silver at these locations. After the "latent image" is processed, the results can be visualized. This process can be time consuming and cumbersome (3).

Phosphor Imaging

Another modality has been developed that operates similarly to emulsion film autoradiography. A sheet with a coating of excitable phosphor crystals is placed atop the sample. Upon exposure, low energy electron-hole pairs are created by the interaction of

the phosphor with the incident radiation. Most recombine and luminescence can be observed locally. However, some of the new electrons become trapped and do not recombine. Upon stimulation with a He-Ne (red) laser, these trapped electrons are freed and find available holes. This creates a violet glow that is observed using fiberoptics. The signal from this system is then amplified by a photomultiplier and then digitized using a scanner (4). Upon review, Kamarainen et al. (2006) found that compared to photostimulated luminescence, "…film autoradiography requires more time for optimizing, preparing, and analyzing films because of poor sensitivity and low linearity" (5).

MicroImager Information

Operating Principles

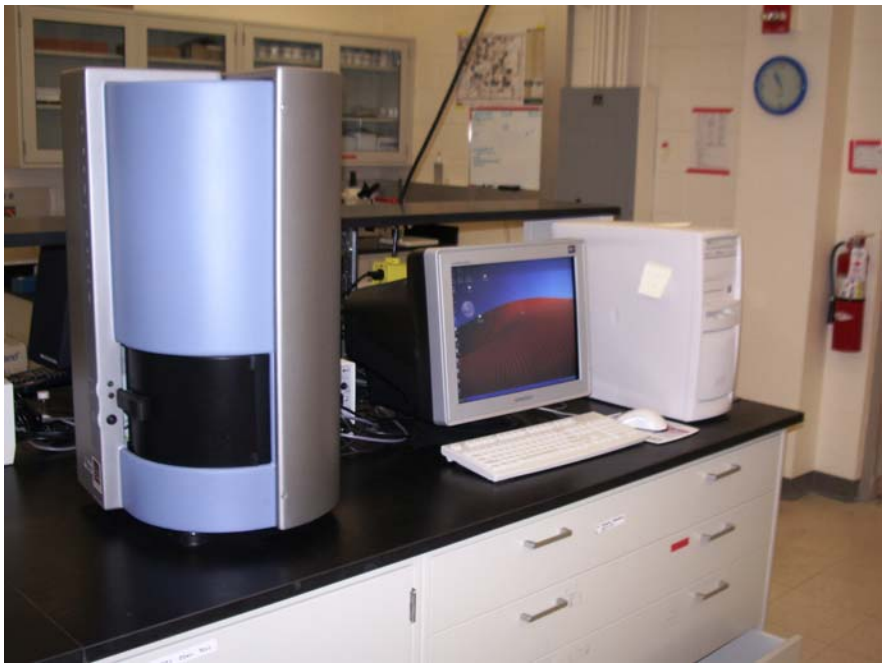

Figure 1. MicroImager with associated PC

The recently developed MicroImager builds on previously developed imaging technology. As the MicroImager is fully digital, no film or phosphor screen is necessary. The sample is placed on a slide and covered with a thin sheet of scintillating paper. This paper converts beta particles to photons. These photons are amplified in an Image Intensifier Tube and enter a CCD Camera. The computer then assimilates the data into an observable image that is displayed to the user. This system has several advantages over traditional imaging modalities. Digital storage of data is more compact, easier to transport, and easier to view than photographic film or phosphor screens. The high-resolution (~20μm) and high speed of data acquisition (on the order of hours) is advantageous compared to previous technology. Additionally, this system can be automated to process up to four samples in one run. High throughput data analysis is valuable because it provides the investigator with time to focus on other tasks while acquiring important data.

The MicroImager also has the unprecedented ability to distinguish two different isotopes in one sample. If isotopes emitting radiation at different energy levels are used (i.e. ^{3}H and ^{14}C), the software can differentiate between the two. Each beta particle will have a different size "light spot" on the screen dependant on its energy. After user standards are prepared, the software can determine the source of each "spot" and assign it to a specific isotope. This can not be done using film emulsions or phosphor imaging.

Hardware Components of MicroImager

Scintillating Sheet

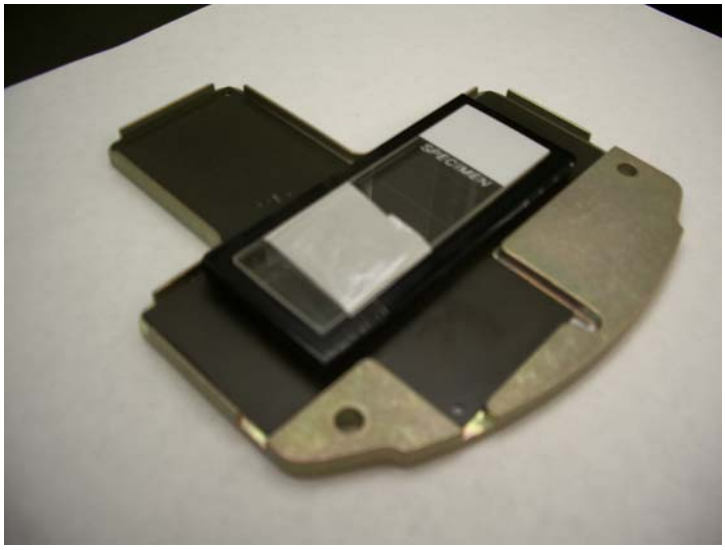

Figure 2. Scintillating sheet on slide

A small, thin sheet of scintillating paper is placed over the sample in order to properly image the sample. The MicroImager employs scintillating sheets made of SiY_2O_5 due to its desired properties (6). The 10 micron thick sheet transforms beta decay from the sample into photons that then move through the image intensifier tube (IIT) on the way to the CCD camera.

Image Intensifier Tube

After the photons are released from the scintillating sheet, they enter the image intensifier tube. This double microchannel plate tube is an optoelectronic device that amplifies the intensity of the incoming light by a factor of 30000 (6). The amplified image is then transferred to a phosphor screen that is lined with an 800 Angstrom aluminized layer. This creates a polarizing current that is picked up by the CCD camera.

CCD Camera

The Charge Coupled Device (CCD) Camera incorporated into the MicroImager has a 576 x 384 pixel screen to integrate incident light. The matrix structure of the CCD camera allows high speed, high resolution images to be acquired. An optical spot is detected by the CCD and then analyzed by an imbedded chip to determine the spot's center of gravity (7). This enables the MicroImager to have a spatial resolution of 15-20 μm. The digital signal created is displayed on the PC screen and can then be processed using Betavision+ software.

Software Components of MicroImager

The images acquired with the MicroImager can then be processed using a dedicated software package called Beta Vision+. This software has broad applications for data analysis and visual interpretation.

Quantification of the data can be conducted in various ways. The final image is a composite of acquisitions done at numerous time points. One can view the entire set of data, or observe only a specific time segment of the acquisition. For example, if the sample was run for 10 hours, one can observe the final image with 10 hours of decay events. On the other hand, one can view the first or last 3 hours of acquisitions. Furthermore, one can observe the middle 5 hours of acquisition. This feature can be valuable for several reasons. First, if decay events should remain constant over time, this can be confirmed by comparing initial acquisition with final acquisition. Secondly, if the radioactive tracer used has a short half-life, one can run the sample and observe the decrease in decay over time. This method enables one to focus on data based on the time

it was obtained. In addition to the temporal distribution, more important data analysis is conducted on the spatial distribution of the signal.

There are several different tools available in Beta Vision+ to aid in spatial analysis of the image. The image of the decay events is acquired using a monochrome camera, yielding a black and white image. The intensity of different locations can be difficult to observe in grayscale images, so pseudocolor can be applied using a preset look-up-table (LUT) or a custom LUT. The range of this scale can be adjusted per user inputs.

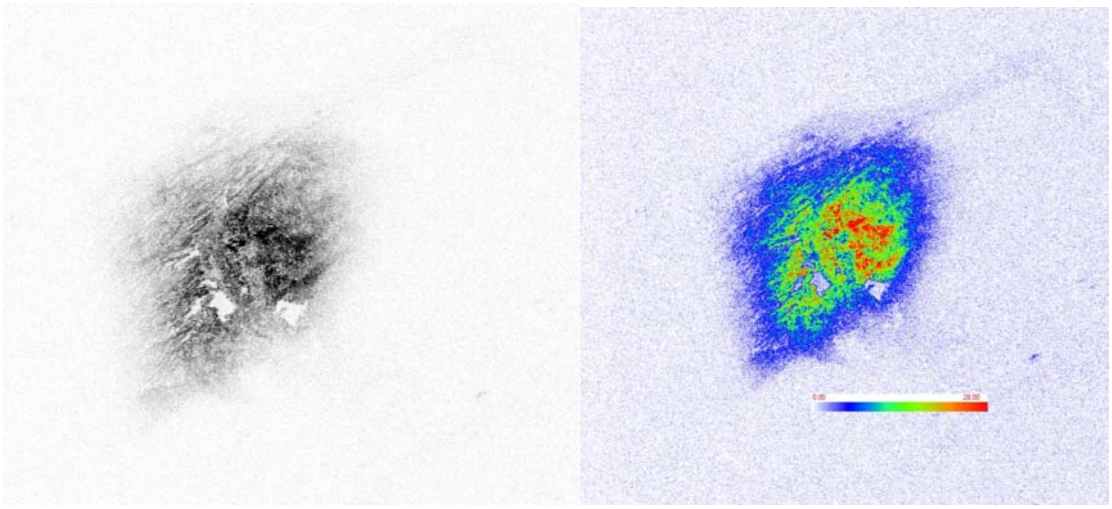

Figure 3. The original autoradiogram of [^{3}H]dexamethasone as acquired by the MicroImager (left) and the same image with a psuedocolor LUT applied (right). The image on the right more clearly shows the variation in intensity

Additionally, there are many other processing and quantitative tools available in the Beta Vision+ software. Among those that will be discussed are the Grid ROI, Circle ROI, Line Profile tool and other tracing tools.

Grid ROI

The Grid Region of Interest (ROI) tool is useful to iteratively analyze a region of the image. After clicking on the Grid ROI icon, the user can input the number of rows and columns desired in the rectangular region. Then, using the mouse, one can draw a grid on the desired area of the image. After this, the Result Viewer can be enabled to display information about each grid square. The data displayed includes the area of each grid and counts within each gridsquare. This data can be exported to other programs such as Excel or Matlab for further analysis.

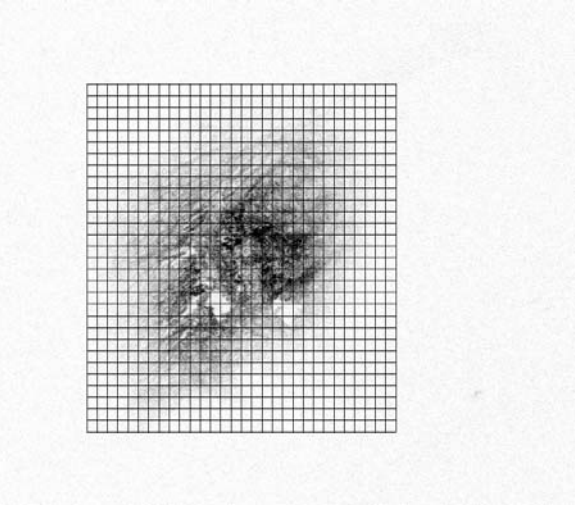

Figure 4. Grid overlay on autoradiogram

Circle ROI

The Circle Region of Interest (ROI) tool can also be used to gather data in specific locations on the image. Several Circle ROI's can be made to radiate from a central point. This is convenient when investigating the radial symmetry of the radioactive tracer. The data attained from individual Circle ROI's can be exported to Excel and processed further.

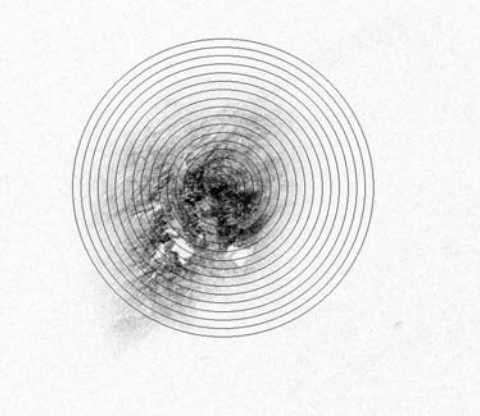

Figure 5. Circle ROI overlay on autoradiogram

Line Profile

Linear characterization of counts can be done using the Line Profile Tool. Upon clicking on the Line Profile tool icon, the user can draw a line of desired length along the image and obtain counts information along this line. The Beta Vision + software measures the counts within a 1 mm width at 0.02 mm intervals along the drawn line. Alternatively, there is another tool available which will measure the counts along a line. This PolyLine tool, however, allows the user to adjust the width of the area being analyzed. These line profile tools are useful for investigating linear distribution of isotope in the sample.

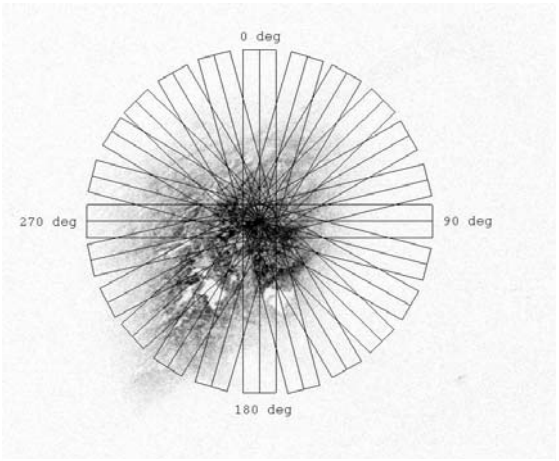

Figure 6. Line Profile on autoradiogram

Tracing

Spatial correspondence to the actual sample is important in order to determine the validity of the data. An optical image can be acquired either prior to, or after radioimaging. This is done by shining an LED light on the sample to obtain an optical density image of the sample. This image is spatially aligned with the autoradiogram because they are both acquired with the same camera without moving the stage or the slide. With the standard package Betavision+ software, one can not directly overlay an optical image with an autoradiographic image. However, using the tracing tools in the measurement toolbar, one can correlate the two images. One can trace an ouline of the

optical image in one window and then "unlink" the trace. After this, one can select the autoradiograph, and the trace will transfer to the other image and be spatially representative of the sample in this image. This is essential for determining the location of isotope in a tissue sample.

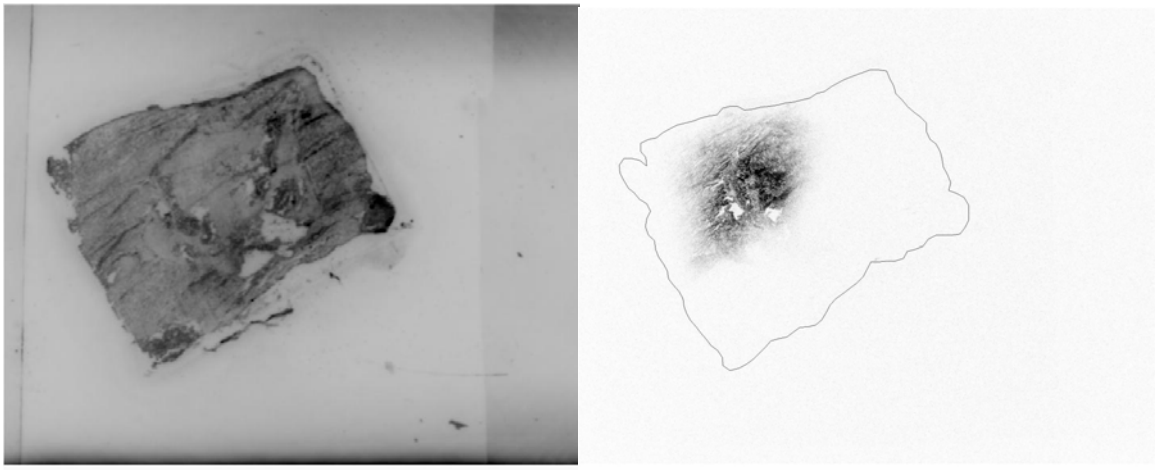

Figure 7. An optical image of rat subcutaneous tissue (left) and the [^{3}H]dexamethasone autoradiogram (right) with a manual trace of the optical image

Previous Applications

The MicroImager is a versatile imaging modality that has been used for a wide array of investigations. Salin et al. (2000) has used the MicroImager to quantitatively analyze the expression of two mRNA species using double isotope *in situ* hybridization (8). They labeled one oligonucleotide with ^{3}H and another with ^{35}S. Their results indicate the MicroImager is capable of accurately discriminating between two different isotopes when used to investigate mRNA expression.

In a different study, Salin et al. (2002) applied the MicroImager to conduct a microarray investigation using ^{3}H and ^{35}S. This study confirmed the high dynamic range and high resolution of the MicroImager are ideal for high density microarray analysis (9).

Our Applications

The investigations conducted in this study evaluate transport characteristics of [^{3}H]dexamethasone in rat subcutaneous tissue. Several experiments were done to determine the elimination constant and diffusion coefficient of dexamethasone in tissue. Different methods were investigated that can be applied to different tissue types in the future. The high speed and high resolution of the MicroImager were critical for the success of these investigations.

Chapter Two

Distribution of [^{3}H]Dexamethasone in Rat Subcutaneous Tissue After Delivery from Osmotic Pumps

Introduction

Several recent reports suggest that controlled local release of dexamethasone may be useful for preventing inflammation around an implantable glucose sensor (10-12). This decrease in inflammation is expected to increase glucose sensor function and lifetime. Local drug delivery may be achieved using biodegradable polymer implants (13), hydrogels (14) and osmotic pumps (15). Local delivery of dexamethasone would permit high interstitial drug concentrations at the site of glucose sensor implantation without producing high systemic drug levels.

For successful local treatment, dexamethasone must be released and penetrate through the tissue surrounding the implanted glucose sensor. Additionally, the concentration of dexamethasone in the subcutaneous tissue surrounding the implanted glucose sensor must be high enough to prevent inflammation to an implant. In a previous study using dexamethasone to suppress inflammation to an implant, local distribution of the drug in subcutaneous tissue was not determined (10). Although dexamethasone is a commonly used anti-inflammatory agent, its local concentration, diffusion coefficient and rate of elimination have not been reported following subcutaneous release. The ability of dexamethasone to penetrate subcutaneous tissue can be measured and quantified by

comparison to mathematical models (13). This method allows a reliable estimate of the drug concentration in the tissue near the implanted glucose sensor.

Experiments were set up to examine the controlled delivery of dexamethasone in normal rat subcutaneous tissue in order to develop a fundamental understanding of how the drug is transported in the subcutaneous tissue. Because the efficacy of controlled interstitial delivery depends on the distance the drug can penetrate into the tissue surrounding the implantable glucose sensor, [^{3}H]dexamethasone was delivered from osmotic pumps that were implanted into the subcutaneous tissue of rats. Digital autoradiographic imaging was used to quantify the spatial distribution of radioactivity in the subcutaneous tissue at 6 hr, 24 hr and 60 hr after subcutaneous implantation. We investigated both the extent of penetration of dexamethasone and the effectiveness of simple transport models for quantification of penetration. From this quantification, the diffusion coefficient of dexamethasone in subcutaneous tissue and the rate of elimination of dexamethasone from the subcutaneous tissue were determined. This information is necessary for the future development of an optimal local delivery system of dexamethasone to reduce the inflammatory response and enhance in vivo sensor function and lifetime.

Materials and Methods

Materials

[^{3}H]dexamethasone (392.46 MW), specifically [1,2,4,6,7-^{3}H]dexamethasone, was obtained from Amersham Biosciences Corp. (Piscataway, NJ). The specific activity

was 88.0 Ci/mmol. Alzet osmotic pumps (1003D model) were obtained from Durect Corp. (Cupertino, CA).

Preparation of Osmotic Pumps

A solution of [^{3}H]dexamethasone and sterile 0.9% (w/v) saline was loaded into the osmotic pumps (total volume 114 μl) using the protocol provided by the manufacturer. Each pump contained a total activity of 127 μCi. The pumps provided a controlled delivery at a rate of 1.0 μL/hr. To prevent the pump from causing a tissue reaction at the site of drug delivery, drug delivery was achieved via a 4 cm length of polyethylene tubing connected to the body of the pump.

Subcutaneous Implantation

Six male Sprague Dawley rats (Harlan, Indianapolis, IN, 375-399 g) were used for our studies. The rats were initially anesthetized by placing each rat in an induction chamber filled with a 5% mixture of isoflurane in oxygen. During surgery anesthetization of the rats was maintained using a 2.5% mixture of isoflurane in oxygen. Two pumps containing radiolabeled dexamethasone were implanted subcutaneously on either side of the shoulders of the rat. A 3-4 cm incision was made between the shoulder blades. A hemostat was inserted into the incision on the lateral aspect. By opening and closing the jaws of the hemostat a pocket in the subcutaneous tissue just large enough for the pump was created. A tunnel to insert the tubing was made using a blunt probe. Excess bleeding was removed with sterile cotton gauze. The osmotic pump was implanted tubing end first. The wound was closed with 4-6 surgical staples.

Two rats were euthanized at 6 hr, 24 hr, and 60 hr after implantation using CO_2. The tissue around the tip of the catheter was removed, quickly frozen on dry ice and stored at -80°C to immobilize the tracers within the tissue sample. The frozen tissue samples were mounted on a cryostat chuck and cut in 10 μm sections. Sections taken at every 200 μm were used for autoradiographic imaging. In addition, sections 50 μm from those sections used for autoradiographic imaging were collected for hematoxylin-eosin (H&E) staining.

All animal experiments were performed under the approval of the University of South Florida Animal Care and Use Program.

Autoradiographic Imaging and Analysis

Autoradiographic images of the tissue sections were obtained using a recently developed real-time digital radioactivity-detection system, the MicroImager (Biospace Mesures, Paris, France) (16, 17). With the MicroImager, acquisition of events can be visualized in real-time on a monitor screen. Each event is individually analyzed by the computer. An event is a radioactivity decay event (16). The acquisition of events need only proceed for as long as is necessary to obtain a good image. In our case, autoradiographic images with between 380,715 to 686,390 events were acquired over 24 to 45 hours to obtain good images. An optical image of the same tissue sample using the MicroImager was also obtained.

The spatial variation in drug concentration from the osmotic pumps was quantified in the following way. The areas of subcutaneous tissue were identified on the optical image and then superimposed onto the corresponding autoradiographic image.

The concentration profiles in the subcutaneous tissue surrounding the catheter tip were determined directly from the autoradiographic images using Beta Vision+ software (Biospace Mesures, Paris, France). A line profile tool (1 mm wide) was used from the center of the catheter tip to the periphery of the subcutaneous tissue to obtain a number of events versus distance profile. The background number of events was subtracted from the number of events acquired. A number of events versus distance profiles were performed at 15° increments around the catheter tip on each section selected for analysis. The number of events at the catheter tip opening was calibrated to the known concentration of the agent in the pump to obtain concentration versus distance profiles at 6 hr, 24 hr and 60 hr after implantation.

Mathematical Model

The concentration profiles of [^{3}H]dexamethasone obtained using the MicroImager were compared to a mathematical model of drug diffusion and elimination. The model assumed: 1) constant drug concentration at the catheter tip/tissue interface; 2) first-order elimination of drug; 3) isotropic diffusional transport of drug through the subcutaneous tissue; 4) negligible fluid convection; and 5) spherical symmetry. The governing equation for the diffusion and elimination of a drug in subcutaneous tissue is:

$$\frac{\partial C}{\partial t} = D\left(\frac{\partial^2 C}{\partial r^2} + \frac{2}{r}\frac{\partial C}{\partial r}\right) - kC \qquad \text{(eq 1)}$$

where C is the concentration of the drug in the subcutaneous tissue, D is the diffusion coefficient of the drug in subcutaneous tissue, r is the radial distance from the center of the catheter tip, k is the first-order elimination constant for the drug from the

subcutaneous tissue and t is the time after implantation. The boundary and initial conditions are:

$$\begin{aligned} &C = 0 && \text{at } t = 0; && r \geq a \\ &C = C_0 && \text{at } t > 0; && r = a \\ &C = 0 && \text{at } t > 0; && r \to \infty \end{aligned} \qquad \text{(eq 2)}$$

where a is the radius of the catheter and C_0 is the concentration at the catheter tip. The solution of eq 1 using the boundary and initial conditions of eq 2 is (22):

$$\frac{C}{C_0} = \frac{a}{2r}\left\{\exp\left[-(r-a)\sqrt{\frac{k}{D}}\right] erfc\left[\frac{r-a}{2\sqrt{Dt}} - \sqrt{kt}\right] + \exp\left[(r-a)\sqrt{\frac{k}{D}}\right] erfc\left[\frac{r-a}{2\sqrt{Dt}} + \sqrt{kt}\right]\right\} \qquad \text{(eq 3)}$$

Assuming steady state, and applying the two boundary conditions from eq 2, eq 1 can be solved using a series solution. Alternatively, the steady state solution can also be found from eq 3 by applying the limit $t \to \infty$:

$$\frac{C}{C_0} = \frac{a}{r}\exp\left[-(r-a)\sqrt{\frac{k}{D}}\right] \qquad \text{(eq 4)}$$

The Brownian diffusion coefficient for dexamethasone in water was estimated from the Stokes-Einstein equation:

$$D = \frac{\kappa T}{6\pi\mu r_s N_A} \qquad \text{(eq 5)}$$

where $r_s = 0.657\ M^{1/3}$ [$x10^{-10}$ m] is the equivalent spherical solute radius, M is the molecular weight of dexamethasone (392.46 MW), κ is the ideal gas constant 8.314 $JK^{-1}mol^{-1}$, T is temperature, μ dynamic viscosity and N_A is Avogadro's number. The calculated diffusion constant of dexamethasone in water at 37°C is $D = 6.82x10^{-10}$ m^2/s. The Stokes-Einstein equation underpredicts the actual diffusion coefficient for small

solutes of molecular weight less than several hundred, and overpredicts it for large solutes of molecular weight greater than several thousand (19).

Measured concentration profiles for [^{3}H]dexamethasone at t = 6 hrs, t = 24 hrs and t = 60 hrs were compared to the transient equation (eq 3). Typical concentration profiles predicted by eq 3 for two values of ϕ for various times are shown in figures 8a and 8b. The dimensionless parameter ϕ, where $\phi = a\sqrt{k/D}$, is analogous to the Thiele

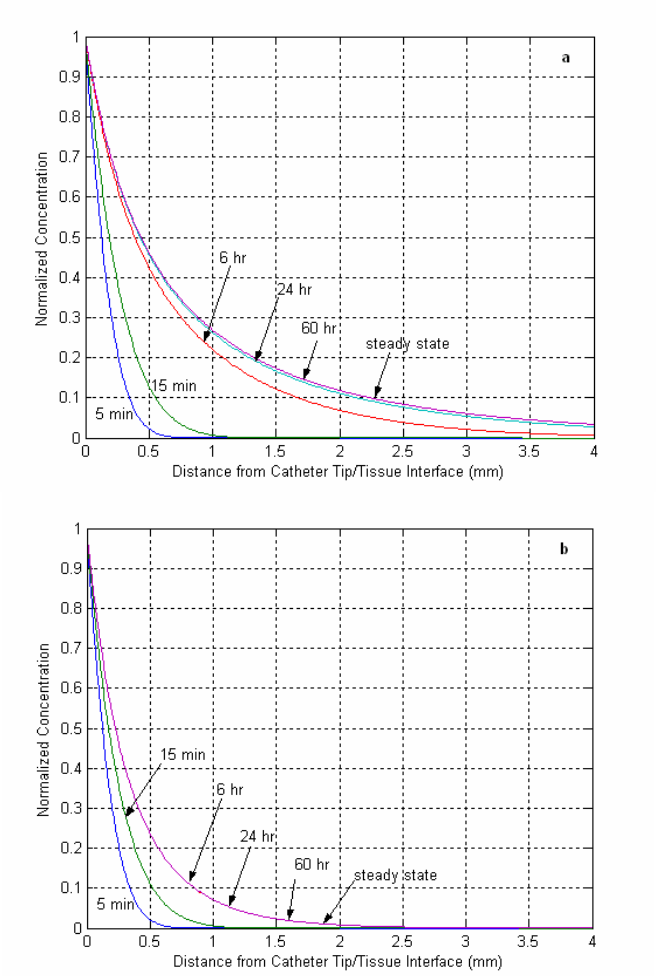

Figure 8. Concentration versus distance profiles obtained by solving the transient diffusion and elimination equation (eq 3) for various times until steady state is reached are shown. Panels a and b demonstrate the dependence of the penetration depth with the modulus $\phi = a\sqrt{k/D}$. Panel a (ϕ = 0.2) has a larger penetration depth than panel b (ϕ = 1)

modulus obtained in analysis of heterogeneous catalysis (13) and is a predictor of the extent of drug penetration from the catheter tip.

The radius of the catheter was approximated at 0.6 mm. Values for D and k were found in the following manner. First, initial estimates for D and k were found. For the initial estimate of D, the diffusion constant for dexamethasone in water was used, D = 6.82×10^{-10} m^2/s. This D was used in the steady-state solution of the diffusion equation (eq 4) to find an initial estimate for k. k was found by using the Marquardt-Levenberg technique (20) with two independent variables, k and C_0, to minimize the residual of the sum-squared-error between the predicted and experimental concentrations. Second, these initial estimates for the k and D values were then used as the starting points for the Marquardt-Levenberg algorithm using the transient equation (eq 3) with the k, D, and C_0 being the three independent variables over which the residual of the sum-squared-error between the predicted and experimental concentrations was to be minimized. The initial value for C_0 was always the maximum concentration in the measured data set. The Marquardt-Levenberg algorithm efficiently searched over the k, D, and C_0 space to find the point which best fits the data (21). This technique was repeated to find k and D for 6 hr, 24 hr, and 60 hr. For each of these times, the calculations were repeated for the autoradiographic scans at various angles. The Marquardt-Levenberg algorithm was written in MATLAB.

Results

Radiolabeled dexamethasone spread through the subcutaneous tissue after implantation of the osmotic pump (fig. 9). The local concentration of drug within the tissue was quantified from the autoradiographic images using the Beta Vision+ software. The Beta Vision+ software was used to construct the number of events as a function of distance profiles. An event is a radioactivity decay event (16). The number of events was greatest at the tip of the catheter. A high number of events on the autoradiographic image represents a high drug concentration. The number of events at the tip of the catheter can be calibrated to the known concentration in the pump. Hence, the local concentration of the drug in the subcutaneous tissue surrounding the catheter can be estimated by comparing the local number of events to the number of events at the catheter tip. In general, at distances more than a few millimeters from the catheter tip, the radioactivity was not significantly different from background. Figure 9 is representative of the autoradiographic images obtained using the MicroImager after implantation of the osmotic pumps for 6 hr, 24 hr, or 60 hr.

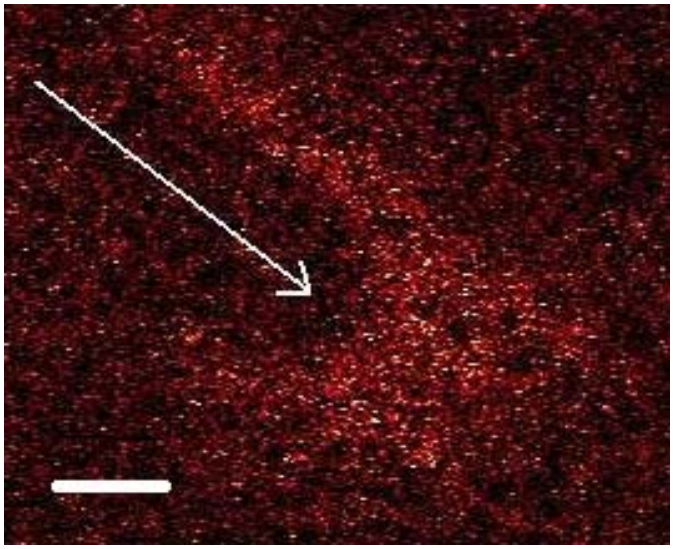

Figure 9. Autoradiographic image from rat subcutaneous tissue obtained using the MicroImager after implantation of an osmotic pump containing [^{3}H]dexamethasone for 6 hrs. The location and direction of the catheter tip is shown by the arrow. Each red dot represents a radioactivity decay event. Lighter shades indicate higher activity. The bar represents a distance of 1 mm.

Concentration profiles obtained from the autoradiographic images of the subcutaneous tissue surrounding the catheter tip were examined and compared to the mathematical model of diffusion and first-order elimination to find the best estimates for D and k.

The best estimates obtained for D and k are given in Table 1. A single-factor analysis of variance (ANOVA) indicated that there was no significant difference between the 6 hr and 24 hr data for k ($p > 0.05$) or for D ($p > 0.05$). There was not enough data at 60 hr for comparison. The average, based on the 6 hr, 24 hr and 60 hr data, for the diffusion coefficient is $D = 4.11 \pm 1.77 \times 10^{-10}$ m^2/s and for the elimination constant is $k = 3.65 \pm 2.24 \times 10^{-5}$ s^{-1}.

Table 1. Estimated D and k

The diffusion coefficient and elimination constant was determined by fitting a model of diffusion and elimination to the concentration profiles measured near the tip of a catheter attached to an osmotic pump.

Time after implantation	n	k [1/s] x 10^{-5}	D [m^2/s] x 10^{-10}
6 hr	5	4.80 ± 2.56	3.63 ± 1.06
24 hr	6	2.52 ± 1.65	4.92 ± 1.97
60 hr[a]	1	4.70	1.73

[a] Only one scan was suitable for analysis in this case, as the subcutaneous tissue was very thin, allowing measurement without boundary effects only in one case.

To quantify differences in drug penetration with time after release from the osmotic pump, the best fit concentration profiles were used to find the distance where the local concentration drops to 10% of its maximum value (figs. 10a, b, c). For the 6 hr case,

the majority of the drug was confined to a region within 2.22 ± 0.42 mm from the tip of the catheter (table 2). For the 24 and 60 hr cases, the majority of the drug was confined to a region within 2.70 ± 0.38 mm and 1.80 mm from the tip of the catheter, respectively. The penetration distance of [^{3}H]dexamethasone increased from 6 hr to 24 hr, but decreased from 24 hr to 60 hr.

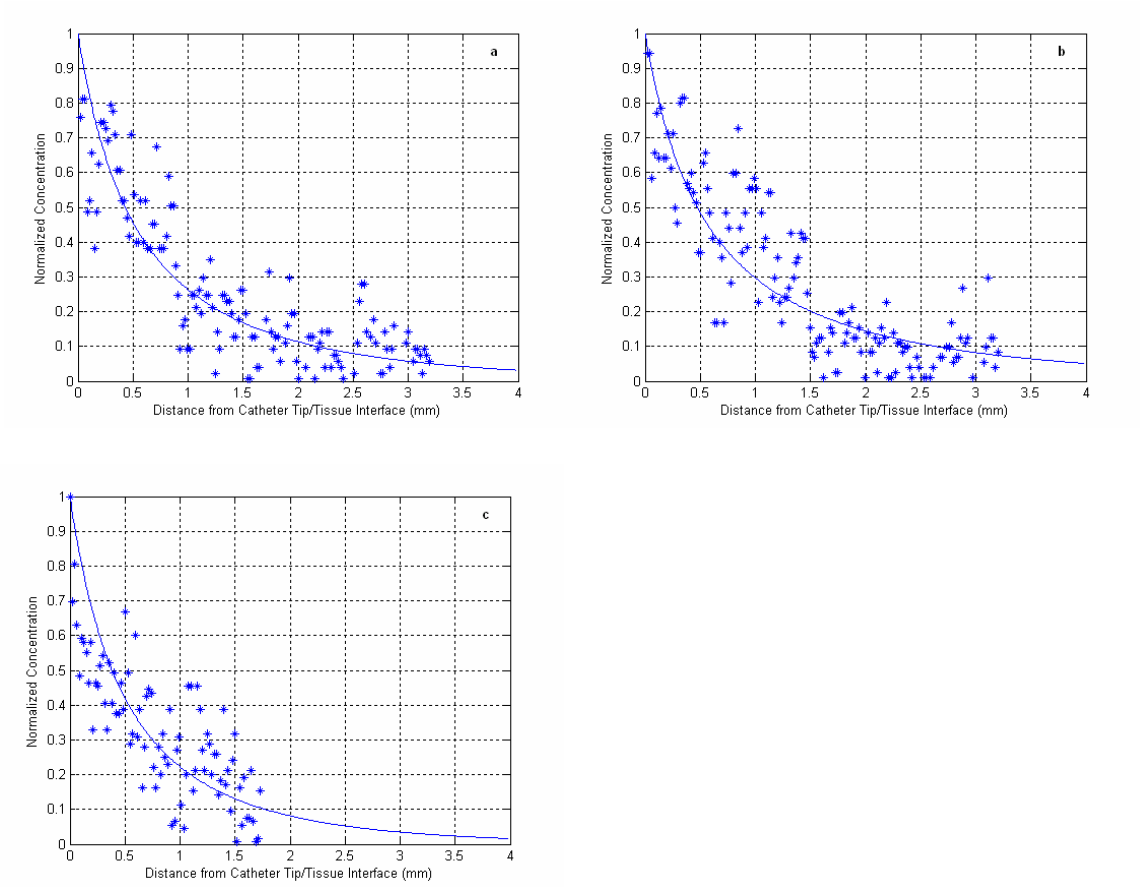

Figure 10. Typical concentration profiles in the vicinity of the catheter tip at (a) 6 hr, (b) 24 hr and (c) 60 hr after implantation. Data from only one angle per time period is shown. Combining data from all. **9**other scans would make the figure unreadable. The solid lines show the transient diffusion and elimination model (which reduces to the steady state model as $t\rightarrow\infty$) in which k, D and C_0 was varied to minimize the residual of the sum-squared-error between the predicted and experimental values. The ordinate represents the location of catheter tip/tissue interface

Table 2. Penetration distance of radioactivity from the tip of the catheter

The penetration distance is the distance where the local concentration drops to 10% of the concentration at the catheter tip. This radial distance was found using the best fit curve through the data and corresponds to the location where $C/C_0 = 0.1$. The dimensionless parameter, $\phi = a\sqrt{k/D}$, determines the extent of drug penetration and was found using the corresponding k and D values in Table 1.

Time after implantation	Penetration Distance [mm]	$\phi = a\sqrt{k/D}$
6 hr	2.22±0.42	0.22
24 hr	2.70±0.38	0.14
60 hr	1.80[a]	0.31

[a] See note on table 1.

Discussion

Radiolabeled dexamethasone was introduced into the subcutaneous tissue by implantation of osmotic pumps. There was constant delivery of the agent from the pump via an attached catheter. High concentrations of the agent were located near the tip of the catheter. The local distribution of the agent in the subcutaneous tissue surrounding the catheter tip was measured and analyzed. The distribution of the agent within the subcutaneous tissue near the catheter tip was consistent with the mathematical model of diffusion and first-order elimination (figs. 10a, b, c). The mathematical model was compared to the experimental data in order to obtain values for the diffusion coefficient D, and the elimination constant k at 6 hr, 24 hr and 60 hr after implantation. The experiment was terminated at the end of 60 hr as the concentration profile reached steady state at 60 hr (fig. 8a) (further discussion below).

The diffusion coefficient, D, of dexamethasone in subcutaneous tissue at 6 hr and 24 hr after implantation was $3.63 \pm 1.06 \times 10^{-10}$ m^2/s and $4.92 \pm 1.97 \times 10^{-10}$ m^2/s, respectively. The 60 hr data suggests a D of 1.73×10^{-10} m^2/s. There was no significant difference between the 6 hr and 24 hr data for D ($p > 0.05$). A comparison with the 60 hr data was not made as the sample size was too small. Even though the concentration profile at 6 hr has not yet reached steady state (fig. 8a), the value found for D should not be different from that found for the 24 hr case which is very close to steady state. (Note that at 6 hr, $\phi = 0.22$ (table 2) and fig. 8a shows concentration profiles for $\phi = 0.2$ for various times.) The concentration profile at 60 hr has reached steady state (fig. 8a). D should have similar values at 6 hr, 24 hr and 60 hr because the best estimate for D and k for all cases was achieved using the transient diffusion and elimination equation (eq 3). Since the transient equation takes time into account, be it for a short time period or for a long time period, the D and k values for the same agent in the same tissue should be the same. D and k are assumed to be constants. As time becomes large, the transient equation (eq 3) reduces to the steady equation (eq 4). Hence, the average diffusion coefficient D = $4.11 \pm 1.77 \times 10^{-10}$ m^2/s based on the 6 hr, 24 hr and 60 hr data, results in a reasonable value for dexamethasone in subcutaneous tissue. The diffusion coefficient of dexamethasone in subcutaneous tissue is slightly less than in water but slightly greater than in brain tissue (table 3). Our diffusion coefficient for dexamethasone in rat subcutaneous tissue is slightly greater than the diffusion coefficient of sodium fluorescein (molecular weight 376) in rat subcutaneous tissue $D = 2.35 \pm 0.24 \times 10^{-10}$ m^2/s (24). Sodium fluorescein has a similar molecular weight as dexamethasone (molecular weight 392).

Table 3. Diffusion coefficients for dexamethasone in various media

The diffusion coefficient of dexamethasone in subcutaneous tissue was compared to the diffusion coefficient for dexamethasone in other media from the literature.

Medium	D [m^2/s]	Reference
water	6.82×10^{-10}	Stokes-Einstein equation
subcutaneous tissue	$4.11 \pm 1.77 \times 10^{-10}$	This study
brain tissue	2.0×10^{-10}	Saltzman and Radomsky, 1991 (22)
cellulose acetate membrane	3.15×10^{-11} [a]	Barry and Brace, 1977 (23)

[a] Interpolated for 37°C

The elimination constant, k, at 6 hr and 24 hr was $4.80 \pm 2.56 \times 10^{-5}$ s^{-1} and $2.52 \pm 1.65 \times 10^{-5}$ s^{-1}, respectively. The 60 hr data suggests a k of 4.70×10^{-5} s^{-1}. There was no significant difference between the 6 hr and 24 hr data for k ($p > 0.05$). A comparison with the 60 hr data was not made as the sample size was too small. The average, based on the 6 hr, 24 hr and 60 hr data, for the elimination constant is $k = 3.65 \pm 2.24 \times 10^{-5}$ s^{-1}. This value is quite reasonable despite the fact that the 6 hr case has not yet reached steady state for the reasons given in the paragraph above. Table 4 shows values for k of other agents in subcutaneous tissue. Our elimination constant for dexamethasone in rat subcutaneous tissue is slightly greater than that of dexamethasone in rat brain $k = 1.19 \times 10^{-5}$ s^{-1} (26).

Although only two rats were used for each time point, we did not observe any variation between the two rats as they were the same age, sex, size, and strain and were all from the same vendor. A detailed study would be useful to demonstrate that the age, sex, size, strain and vendor have no significant effect on the values of D and k. However, this extensive work is beyond the scope of this paper.

Table 4. Elimination constants of various agents in subcutaneous tissue

The elimination constant of dexamethasone in subcutaneous tissue was compared to the elimination constant of other agents in subcutaneous tissue from the literature.

Agent	k [1/s]	Reference
RSA[a]	$6.42 \pm 1.19 \times 10^{-5}$	Kim and Burgess (2002) *(16)*
Dexamethasone	$3.65 \pm 2.24 \times 10^{-5}$	This study
VEGF[b]	$3.50 \pm 1.03 \times 10^{-5}$	Kim and Burgess (2002) *(16)*

[a] rat serum albumin
[b] vascular endothelial growth factor

Dexamethasone penetrated an average distance of 2.22 ± 0.42 mm at 6 hr, 2.70 ± 0.38 mm at 24 hr and 1.80 mm at 60 hr into the subcutaneous tissue near the implant (table 2). The difference between the penetration distances at 6 hr and 24 hr is most likely due to the fact that at 6 hr steady state has not yet been reached and hence, the furthest extent of drug penetration has not yet been reached (fig. 8a). The reduction in penetration distance at 60 hr compared to that at 24 hr may be explained from an analysis of the H&E stained slides. Histopathological evaluation of the slides revealed that there were more inflammatory cells at 60 hr than for 24 hr after implantation. It should be noted that the actual amount of [^{3}H]dexamethsone used for this study was very small. This amount of [^{3}H]dexamethasone after 60 hr of delivery resulted in slightly less than the maximum amount of radioactivity allowed in an animal for normal disposal. This small amount of dexamethasone would not have had a significant effect on the number of inflammatory cells. The number of inflammatory cells may have affected the transport characteristics. Kim et al. (25) also suggested that the body's inflammatory response to local delivery devices located at a subcutaneous site may complicate drug release.

The average ϕ, based on the average values for D and k, is ϕ = 0.18. Since D and k values for the same agent in the same tissue are assumed to be constants, then $\phi = a\sqrt{k/D}$ must also be a constant. Although the modulus ϕ determines the extent of drug penetration, the penetration distance for a given ϕ may be different at different times (figs. 8a, b). The maximum extent of drug penetration is not reached until steady state is reached. At times prior to steady state, the penetration distance is less then maximum. In general, the penetration distance increases as ϕ decreases (figs. 8a, b) because the rate of diffusion is greater than the rate of elimination. The modulus ϕ is useful in predicting the extent of drug penetration between different drugs at steady state.

The model also assumed isotropic diffusional transport of drug through the subcutaneous tissue. Figure 11 shows a typical H&E stained tissue section from our study. The subcutaneous tissue was homogeneous. Hence, the assumption that the tissue would be isotropic for diffusional transport seems reasonable.

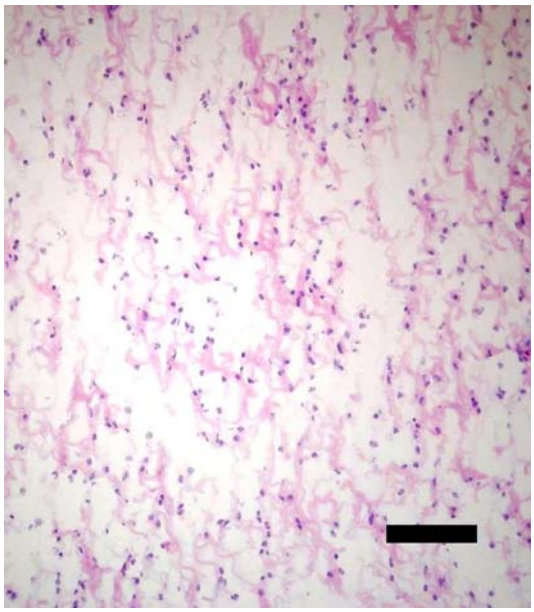

Figure 11. A typical H&E stained tissue section from our study. The bar represents a distance of 100 μm

Our model of drug distribution within the subcutaneous tissue assumes that drug transport occurs predominately by diffusion. The Peclet number (Pe = *v*a/D), where *v* is the velocity of the dexamethasone solution in the tissue and *a* is the radius of the catheter, was 0.18. Hence, this assumption is acceptable.

The model assumed spherical symmetry, although the delivery of drug was from a pipe. As the model was consistent with the data (figs. 10a, b, c), this assumption appears to be acceptable.

From other experiments in our laboratory, we have determined the minimum dosage of dexamethasone that would prevent inflammation to a glucose sensor implanted subcutaneously. This dosage was found to be 0.12 mg per day (unpublished data). Knowledge of this minimum value along with the values of the diffusion coefficient and elimination constant found in this study, one can design an effective and efficient local drug delivery system around any implantable glucose sensor or implant whose function is affected by inflammation.

Chapter Three

Diffusion of [^{3}H]Dexamethasone in Rat Subcutaneous Slices after Injection Measured by Digital Autoradiography

Introduction

Many transport experiments are based on the injection of a finite volume of substance into the tissue of interest which then diffuses away. Some examples of injection based diffusion experiments are: the determination of the diffusion coefficient of small molecules in the brain (27); the determination of the diffusion coefficient of growth factors in the brain (28); and the determination of the diffusion coefficient of drugs in tumors (29, 30). Knowledge of the diffusion of a substance of interest in the tissue of interest is important for treatment efficacy. In this paper, we will derive a method in which the diffusion coefficient of an injected substance in tissue can be determined in a relatively simple manner. We will illustrate this technique by finding the diffusion coefficient of [^{3}H]dexamethasone in rat subcutaneous slices after an injection.

Materials and Methods

Materials

[^{3}H]dexamethasone (392.46 MW), specifically [1,2,4,6,7-^{3}H]dexamethasone, was obtained from Amersham Biosciences Corp. (Piscataway, NJ). The specific activity was 88.0 Ci/mmol.

Subcutaneous Injection

Three male Sprague Dawley rats (Harlan, Indianapolis, IN, 375-399 g) were used for our studies. The rats were euthanized using CO_2 prior to the experiment.

The 20 minute experiment: Three 40 µl solutions of [^{3}H]dexamethasone in sterile 0.9% (w/v) saline were used. Injections were made into subcutaneous tissue. Each solution contained a total activity of 0.65 µCi. The tissue around the injection site was removed and frozen on dry ice. The average time from injection to when the tissue froze, as measured using a surface thermometer (Mannix Testing & Measurement, Lynbrook, NY), was approximately 20 minutes after injection.

The 157 second experiment: Three subcutaneous sections were harvested. Each section was injected with 40 µl solutions of [^{3}H]dexamethasone in sterile 0.9% (w/v) saline and then frozen on dry ice. The average time from injection to when the tissue froze was approximately 157 seconds after injection.

All tissue samples were then stored at -80°C to immobilize the tracers within the tissue sample. The frozen tissue samples were mounted on a cryostat chuck and cut in 10 µm sections. Sections taken at every 200 µm were used for autoradiographic imaging.

All animal experiments were performed under the approval of the University of South Florida Animal Care and Use Program.

Autoradiographic Imaging and Analysis

Autoradiographic images of the tissue sections were obtained using a real-time digital radioactivity-detection system, the MicroImager (Biospace Mesures, Paris, France) *(16, 17).* With the MicroImager, acquisition of events can be visualized in real-

time on a monitor screen. The acquisition of events needs only to proceed for as long as is necessary to obtain a good image. In our case, autoradiographic images with between 1,593,815 to 1,918,869 events were acquired over 71 h 32 min to 72 hr 43 min to obtain good images.

The spatial variation in drug concentration from the injection was quantified as follows. A grid was placed over the autoradiographic image using the Beta Vision + software (Biospace Mesures, Paris, France) to determine the number of events in each 0.3 x 0.33 mm grid area. The grid area that contained the highest number of events (or greatest radioactivity) was taken to be the center of the injection. The concentration profiles versus distance in the subcutaneous tissue surrounding the center of injection were determined directly from the autoradiographic images using the Beta Vision+ software (Biospace Mesures, Paris, France). A line profile tool (1 mm wide) was used from the center of the injection to the periphery of the subcutaneous tissue to obtain a number of events versus distance profile. The background number of events was subtracted from the number of events acquired. The number of events can be calibrated to concentration.

Mathematical Model

The concentration profiles of [^{3}H]dexamethasone obtained using the MicroImager were compared to a mathematical model of drug diffusion. The model assumed 1) that the diffusing substance is deposited within a sphere of radius a at t = 0; 2) isotropic diffusional transport of drug through the subcutaneous tissue; 3) negligible fluid convection; and 4) negligible elimination. Assuming that the elimination is negligible is justified as tissue samples were obtained from a sacrificed rat. That is, the absence of

blood flow eliminates most clearance mechanisms normally present *in vivo* (28). Hence, the governing equation for diffusion of a drug in the subcutaneous tissue is:

$$\frac{\partial C}{\partial t} = \frac{D}{r^2}\frac{\partial}{\partial r}\left(r^2 \frac{\partial C}{\partial r}\right) \qquad \text{(eq 6)}$$

where C is the concentration of the drug in subcutaneous tissue, D is the diffusion coefficient of the drug in subcutaneous tissue, r is the radial distance from the center of the injection and t is the average time from injection to when the tissue froze. The initial concentration is C_o in the sphere, $0 \le r < a$ and zero for $r > a$. The boundary conditions is $C(\infty, t) = 0$. The analytic solution for eq 6 using the above initial and boundary conditions is *(18, 31)*:

$$C = \frac{1}{2}C_o\left\{erf\,\frac{r+a}{2(Dt)^{1/2}} - erf\,\frac{r-a}{2(Dt)^{1/2}} - \frac{2(Dt)^{1/2}}{r\pi^{1/2}}\left[e^{-(r-a)^2/4Dt} - e^{-(r+a)^2/4Dt}\right]\right\} \qquad \text{(eq 7)}$$

where a is the radius of the sphere.

If $r >> a$, then expression (eq 7) becomes (18):

$$C = \frac{m}{8(\pi Dt)^{3/2}} e^{-\frac{r^2}{4Dt}}\left\{1 + \left(\frac{r^2}{Dt} - 6\right)\frac{a^2}{40Dt}\right\} \qquad \text{(eq 8)}$$

where $m = VC_o = 4/3\pi a^3 C_o$, and V is the injected volume.

If the radius of the sphere tends to zero, $a \to 0$, with m remaining constant (18):

$$C(r,t) = \frac{m e^{-\frac{r^2}{4Dt}}}{8(\pi Dt)^{3/2}} \qquad \text{(eq 9)}$$

or $$\frac{C(r,t)}{C_o} = \frac{a^3 e^{-\frac{r^2}{4Dt}}}{6\pi^{1/2}(Dt)^{3/2}} \qquad \text{(eq 10)}$$

Equation 9 is the same solution as for the instantaneous point source in 3D (32). However, Nicholson (33) suggests that at measurement locations sufficiently far from the source, eq 9 (or eq 10) will provide a useful approximation. Moreover, Thorne et al. (28) suggest that when the injection time is very brief compared to the time of the subsequent diffusion measurements, the concentration can be described by eq 9 (or eq 10).

Typical concentration profiles for [^{3}H]dexamethasone predicted by eq 10 at t = 2.5 min, t = 5 min, t = 10 min, and t = 20 min are shown in Figure 12.

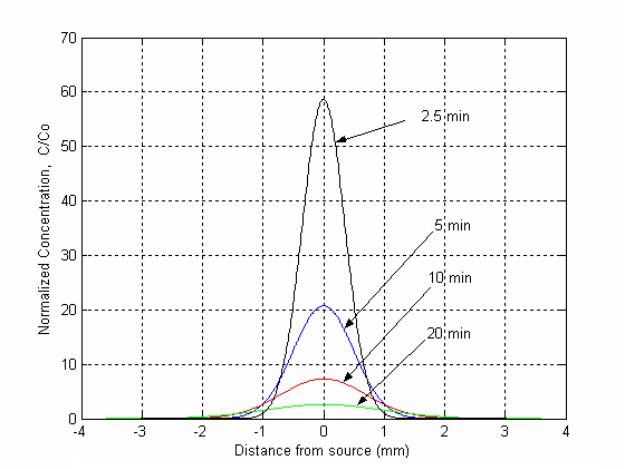

Figure 12. Concentration profiles for diffusion when a concentrated bolus of solute is deposited within a small region. The curves shown are a realization of eq 5 with $D = 4.11 \times 10^{-10}$ m^2/s, a = 0.21 cm, and t = 2.5 min, 5 min, 10 min, and 20 min

The radius of the injected spherical volume was 2.1 mm. For eq 5 to be a useful approximation, data away from the source was used (33). For the 20 min experiment, a portion of the concentration profile from the tail-end was used in the mathematical model. This portion ranged from the tail-end to a position 3 mm towards the source from the first zero event value. For the 157 s experiment, first zero event value could not be used as reference point. Instead, a location on the profile where the profile "bends" from a steep curve to a plateau region was used as a reference. This "bend" was defined to occur at a position where the number of events was 100. Therefore, the portion of the concentration profile used in the mathematical model was from the tail-end to a distance 0.7 mm towards the source after the "bend". The reason that the first zero event value could not be used as a reference

point will be discussed further in the discussion section below. The value for D was found in an iterative manner. First, an initial estimate for D was needed. The diffusion constant for dexamethasone in water was used, $D = 6.82 \times 10^{-10}$ m^2/s (34). This initial estimate for D was then used as the starting points for the Marquardt-Levenberg algorithm (20) with the D, and C_0 being the two independent variables over which the residual of the sum-squared-error between the predicted and experimental concentrations was to be minimized. The initial value for C_0 was always the maximum concentration in the measured data set. The Marquardt-Levenberg algorithm efficiently searched over the D, and C_0 space to find the point which best fits the data (21). This technique was repeated to find D for 157 s and 20 min. For each of these times, the calculations were repeated for the autoradiographic scans at various angles. The Marquardt-Levenberg algorithm was written in MATLAB.

Results

Radiolabeled dexamethasone spread through the subcutaneous tissue after injection. Figure 13 is representative of the autoradiographic images obtained using the MicroImager after injection of a radiolabeled drug. The local concentration of drug within the tissue was quantified from the autoradiographic images using the Beta Vision+ software. The Beta Vision+ software was used to construct the number of events as a function of distance profiles. Figure 14 is representative of the number of events versus distance profiles obtained from the autoradiographic images. An event is a radioactivity decay event (16). The number of events was greatest at the center of the injection. A high number of events on the autoradiographic image represent a high drug concentration. The

number of events can be calibrated to concentration to obtain concentration versus distance profiles.

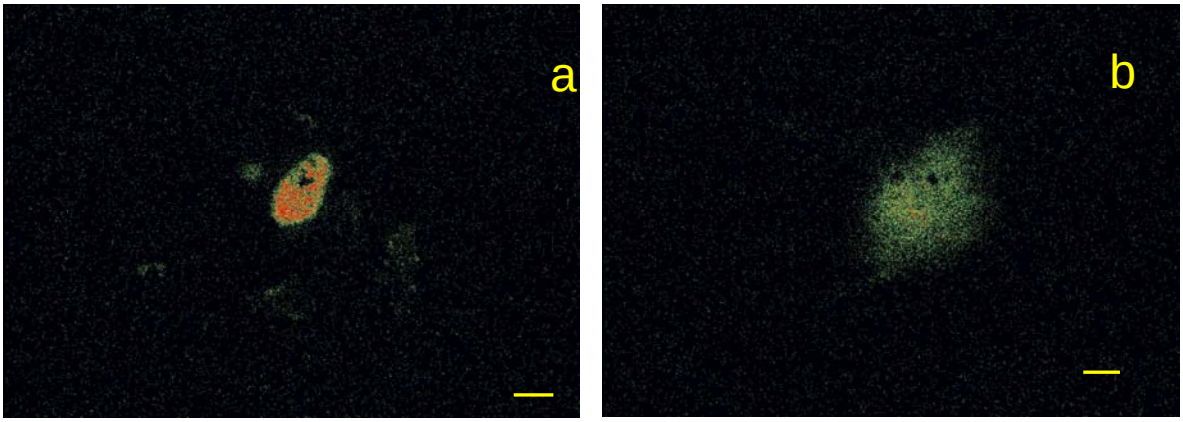

Figure 13. Image a shows a typical autoradiographic image obtained using the MicroImager 157 s after injection of [^{3}H]dexamethasone. Image b shows an autoradiographic image 20 min after injection of [^{3}H]dexamethasone. Red indicates higher activity than green. The bar represents a distance of 2 mm

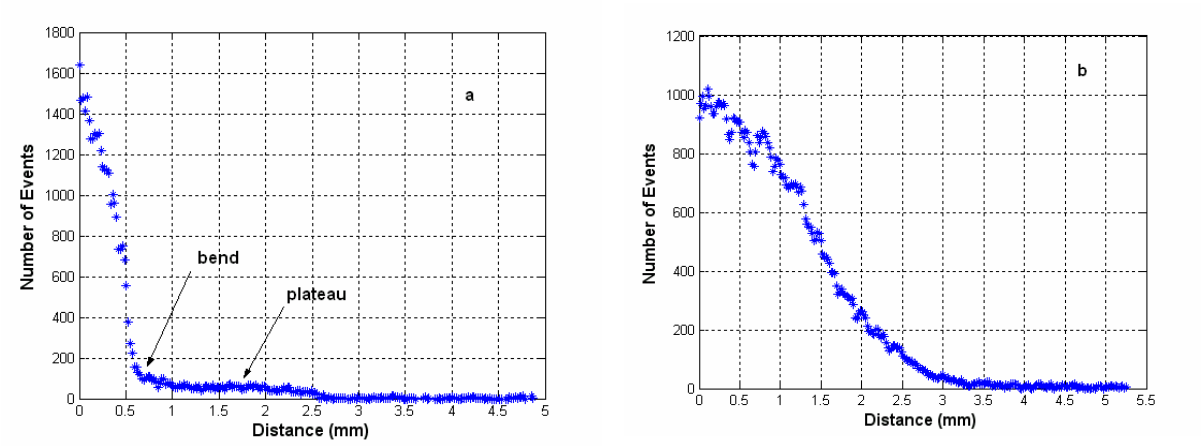

Figure 14. Typical number of events versus distance profiles obtained using the MicroImager at (a) 157 s and (b) 20 min after implantation. Data from only one scan is shown. Combining data from all other scans would make the figure unreadable. The ordinate represents the location of the center of injection

For the 20 min case, the concentration profile from the tail-end to 3 mm towards the source was compared to the mathematical model of diffusion to find the best estimate for D. For the 157 s case, the concentration profile from 0.7 mm towards the source from the "bend" to the tail-end was compared to the mathematical model of diffusion to find the best estimate for D. The best estimates obtained for D are given in Table 5.

Table 5. Estimated diffusion coefficient

The diffusion coefficient was determined by fitting a model of diffusion to the concentration profiles from the tail-end of the profiles.

Time after Injection	n	D [m^2/s] x 10^{-10}
157 s	18	2.68 ± 1.08
20 min	22	4.01 ± 2.01

Discussion

When a substance is injected into tissue in a period that is effectively instantaneous it may exhibit two distinct behaviors: 1) form a fluid-filled cavity; or 2) infiltrate the extracellular space of the tissue (33). The subsequent diffusion from each case can be described by its own set of expressions (33). In this study, we have assumed that the substance does not form a cavity but infiltrates the extracellular space and then diffuses away and hence, have used the appropriate solutions and their approximations for this case.

The approximations to the case where substance infiltrates the extracellular space lead to eq 10. The two criteria for eq 10 to provide a useful approximation are: 1) that the measurement locations be sufficiently far from the source (33); and 2) that the injection

time is very brief compared to the time of the subsequent diffusion measurements (28). To comply with criteria 1, the data near the tail-end of the concentration profiles was used as described below. The measurement distance was kept as small as possible while large enough to provide meaningful data. To investigate criteria 2, two diffusion times were chosen t = 157 s and t = 20 min.

For our study, radiolabeled dexamethasone was introduced into the subcutaneous tissue by injection. Highest concentrations of the agent were assumed to be the location of the center of the injection. This assumption is supported by our theoretical curves (Figure 12). The local distribution of the agent in the subcutaneous tissue surrounding the center of injection was measured (Figure 14).

The local distribution of the agent at the tail end of the distribution was compared to the mathematical model of diffusion. For the 20 min case, the mathematical model was compared to the local distribution from the tail-end to a distance 3 mm towards the center of the injection from the first zero event value. For the 157s case, the mathematical model was compared to the local distribution from the tail-end to a distance 0.7 mm towards the center of the injection from a "bend". The concentration profile "bends" from a steep curve to a plateau region. The "bend" was defined to be the position where the number of events had a value of 100 (see Figure 14a). The plateau region was defined as having a relatively flat profile where the events values where between 0 and 100. The position of the first zero event value could not be used as a reference as the plateau region varied greatly in length. Hence, it would not be possible to set a specified measurement distance from the first zero event value. A plateau region was not seen with the 20 min data.

The distribution of the agent within the subcutaneous tissue at the tail-end of the concentration profile was consistent with the mathematical model of diffusion (Figure 15). The mathematical model was compared to the experimental data in order to obtain values for the diffusion coefficient D at 157s and 20 min after injection.

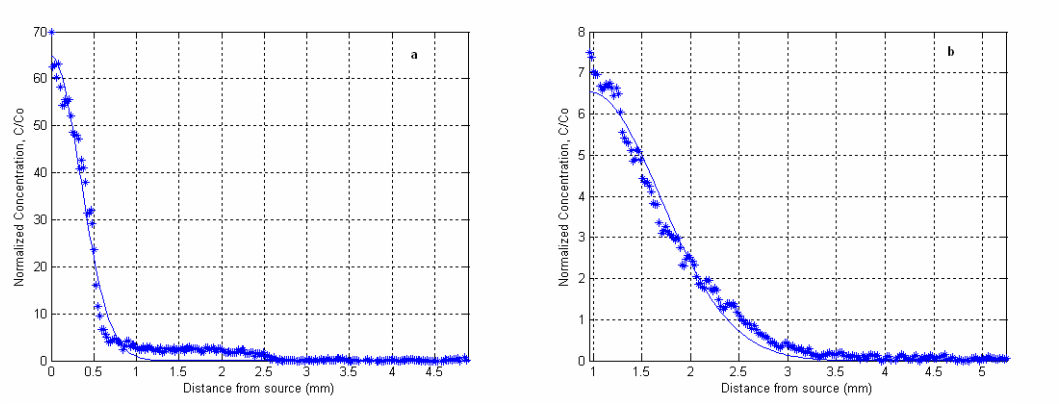

Figure 15. Concentration profiles at the tail-end at (a) 157 s and (b) 20 min after injection. Data from only one angle per time period is shown. Combining data from all other scans would make the figure unreadable. The solid lines show the diffusion model in which D and C_0 was varied to minimize the residual of the sum-squared-error between the predicted and experimental values

The diffusion coefficient, D, of dexamethasone in subcutaneous tissue slices at 157 s and 20 min after injection was $2.69 \pm 1.08 \times 10^{-10}$ m^2/s and $4.01 \pm 2.01 \times 10^{-10}$ m^2/s, respectively.

As mentioned above, there were two criteria for eq 10 to provide a useful approximation. To comply with criteria 1, the data near the tail-end of the concentration profiles was used. However for a few of the concentration profiles for the t = 157 s case, using data 0.7 mm towards the source from the "bend" meant using all the data as the profile was very steep (Figure 15a). Hence, criteria 1 for t = 157 s could not be complied with. For the 20 min case, there was an offset ranging from 0.77 mm to 2.25 mm from the

center of the injection. Although this offset is not large, it may be sufficient enough to comply with criteria 1. In addition, data in Nicholson (33) show that the accuracy of eq 10, at measurement distances close to the source, increases with time.

Criteria 2 required that the injection time be very brief compared to the time of the subsequent diffusion measurements. Although the injection time was not measured, the injection of 40 μl of substance was very brief. The two diffusion times were t = 157 s and t = 20 min. The t = 157 s concentration profile had a plateau region that was not seen in the t = 20 min concentration profile. It could be that at t = 157 s, the injected substance formed both a fluid-filled cavity and infiltrated the extracellular space to some degree producing the plateau region. If this is the case, then eq 10 would not be the appropriate expression. This is a phenomenon that needs to be investigated further and is beyond the scope of this study. The concentration profile at t = 20 min is similar in shape to the theoretical curves realized by using eq 10 (Figure 12), whereas the concentration profile for the t = 157 s is not similar due to the plateau region. Hence, we will assume that for t = 157 s the diffusion time was not long enough and that eq 5 does not provide a useful approximation in this case. A diffusion time of t = 20 min probably provides an adequate diffusion time and hence, eq 10 does provide a useful approximation.

Therefore, the best estimate for the diffusion coefficient of dexamethasone in subcutaneous tissue slices based on the t = 20 min data is $D = 4.01 \pm 2.01 \times 10^{-10}$ m^2/s. We previously found a diffusion coefficient, $D = 4.11 \pm 1.77 \times 10^{-10}$ m^2/s, for dexamethasone in subcutaneous tissue using different experimental and mathematical techniques (34). The diffusion coefficient was determined by fitting a model of diffusion and elimination to the concentration profiles measured near the tip of a catheter attached

to an osmotic pump containing [^{3}H]dexamethasone that was implanted in rats for 6 h, 24 h and 60 h (34). These values for D are very similar suggesting that eq 10 provide an adequate approximation as long as the two criteria are met.

Our mathematical model assumed that the diffusing substance was deposited within a sphere at t = 0. Figure 13a shows the shape of the injection at 157 s is relatively spherical. Hence, the assumption that the injected volume at t = 0 was spherical is acceptable.

The mathematical model also assumed isotropic diffusional transport of drug through the subcutaneous tissue. Figure 13b shows the diffusion of the drug at t = 20 min and diffusion is relatively spherical away from the site of injection. Hence, our assumption of isotropic diffusional transport is reasonable.

The elimination constant was assumed to be negligible as the injections were made in either harvested subcutaneous tissue or in a euthenized rat so that the normal clearance processes that depend on circulation of blood was eliminated (33). In vivo concentration distributions are more complex and neither diffusion nor elimination can be neglected.

In conclusion, eq 10 provides an adequate approximation for measurement locations sufficiently far from the source and for diffusion times much longer than the injection time (28, 33). The main advantages of this injection technique to determine an approximation for the diffusion coefficient are that it is relatively simple technique, and can be applied to any radiolabeled substance of interest injected into any tissue of interest.

Chapter Four

Summary and Future Work

MicroImager

The MicroImager is a highly sensitive autoradiographic imaging modality open to various applications. While the machine is expensive, the cost of obtaining each image is low and can be done quickly. A tissue sample is placed on a slide and covered with a sheet of scintillating paper. This is placed in the machine then autoradiography is performed. The PC associated system stores the data digitally and is easily accessible for storage and processing. This autoradiographic machine can also be used to evaluate the distribution of two different isotopes in a sample.

Osmotic Pump

Tritium labeled dexamethasone was placed within osmotic pumps and implanted into several Sprague Dawley rats. The implants were removed at several time intervals and surrounding tissue was obtained for evaluation. Samples were imaged using the MicroImager and spatial distribution of the radiolabeled dexamethasone was obtained. Mathematical models were created and best fit to experimental results. Using curve fitting, the diffusion coefficient and elimination constant of dexamethasone in subcutaneous tissue were obtained.

Injection Study

Tritium labeled dexamethasone was injected into rat subcutaneous tissue to determine its behavior. After injection, the tissue was explanted and frozen very quickly. Two time points were tested as 2.5 min and 20 min. Mathematical models were obtained and matched to the experimental distribution curves. This study developed a new method to obtain the diffusion coefficient of dexamethasone in any rat subcutaneous tissue. This method can also be applied to different drugs in different tissues.

Possible Future Work

The MicroImager is a versatile imaging modality with many possible applications. Building on this research, experiments can go forward to evaluate receptor-ligand interactions in the brain. For example, [^{3}H]nicotine can be used to label nicotine receptors in the brains of adult and adolescent rats to investigate adolescent vulnerability to nicotine addiction (Moussy and Wecker, personal communication). In addition, future work can also investigate the dual imaging capability of this machine. Some work has already been done investigating this capability. [^{3}H]glucose and ^{14}[C]dextran were used to investigate the permeability of blood vessels (not published). While minimal results were obtained, this study will be useful in preparing future investigations using dual labeling. Future work may include using radiolabeled drugs for the treatment of brain tumors while simultaneously monitoring the metabolism at this site using radiolabeled glucose.

References

(1) Rogers, Andrew W. *Techniques of Autoradiography*. Elsevier Scientific Publishing Company. Amsterdam, (1973).

(2) Herz, R. H. *The Photographic Action of Ionizing Radiations in Dosimetry and Medical, Industrial, Neutron, Auto- and Microradiography*. Wiley-Interscience. New York, (1969).

(3) Baker, John R. J. *Autoradiography: A Comprehensive Overview*. Oxford University Press, Royal Microscopical Society. (1989).

(4) Barnea, Gideon. Detective Quantum efficiency of a storage phosphor imaging plate: Monte Carlo study and experimental results. *14th IEEE International Pulsed Power Conference.* (2003) 82-85.

(5) Kamarainen, Eeva-Liisa, Haaparanta, Merja, Siitari-Kauppi, Marja, Koivula, Teija, Lipponen, Tiina, Solin, Olof. Analysis of ^{18}F-labelled synthesis products on TLC plates: Comparison of radioactivity scanning, film autoradiography, and a phosphoimaging technique. *Appl Radiat and Isot*. (2006) 64 1043-1047.

(6) Laniece, P., Charon, Y., Dumas, S., Mastrippolito, R., Pinot, L., Tricoire. H., Valentin, L., HRRI: A High Resolution Radioimager for Fast, Direct Quantification in In Situ Hybridization Experiments. *Biotechniques* (1994) 17 (2), 338-345.

(7) MicroImager Manual. Biospace Mesures. (2003).

(8) Salin, Helene, Maitrejean, Serge, Mallet, Jacques, Dumas, Sylvie. Sensitive and Quantitative Co-detection of two mRNA species by double radioactive in situ hybridization. *J Histochem Cytochem*. (2000) 48, 1587-1591.

(9) Salin, H., Vujasinovic, T., Mazurie, A., Maitrejean, S., Menini, C., Mallet, J., Dumas, S., A Novel Sensitive Microarray approach for differential screening using probes labeled with two different radioelements. *Nucleic Acids Res*, (2002) 30 (4), e17:1-7.

(10) Hickey, T.; Kreutzer, D.; Burgess, D.J.; Moussy, F. In vivo evaluation of a dexamethasone/PLGA microsphere system designed to suppress the inflammatory tissue response to implantable medical devices. *J. Biomed. Mater. Res*. (2002) 61, 180-187.

(11) Wisniewski, N.; Moussy, F.; Reichert, W. M. Characterization of implantable biosensor membrane biofouling. *Fresenius' J. Anal. Chem*. (2000) *366*, 611-621.

(12) Norton, L. W.; Tegnell, E.; Toporek, S. S.; Reichert, W. M. In vitro characterization of vascular endothelial growth factor and dexamethasone releasing hydrogels for implantable probe coatings. *Biomaterials*. (2005) *26*, 3285-3297.

(13) Strasser, J. F.; Fung, L. K.; Eller, S.; Grossman, S. A.; Saltzman, W. M. Distribution of 1,3-bis(2-Chloroethyl)-1-Nitrsourea and tracers in the rabbit brain after interstitial delivery by biodegradable polymer implants. *J. Pharmacol. Exp. Ther.* (1995) *275*, 1647-1655.

(14) Kurisawa, M.; Chung, J. E.; Yang, Y. Y.; Gao, S. J.; Uyama, H. Injectable biodegradable hydrogels composed of hyaluronic acid-tyramine conjugates for drug delivery and tissue engineering. *Chem. Commun. (Camb).* (2005) *34*, 4312-4314.

(15) Huang, T.S. Concomitant infusion of ovine corticotrophin-releasing hormone does not prevent suppression of the hypothalamus-pituitary-adrenal axis by dexamethasone in male rats. *J. Endocrinol. Investig*. (1997) *20(7),* 393-396.

(16) Rapkin, E. Real-time radioimaging of biological tissue sections. *Am. Biotechnol. Lab*. (2001) *19*, 34-36.

(17) Laniece, P.; Charon, Y.; Cardona, A.; Pinot, L.; Maitrejean, S.; Mastrippolito, R.; Sandkamp, B.; Valentin, L. A new high resolution radioimager for the quantitative analysis of radiolabelled molecules in tissue section. *J. Neurosci. Methods*. (1998) *86*, 1-5.

(18) Carslaw, H. S.; Jaeger, J. C. *Conduction of Heat in Solids, Second Edition*. Oxford University Press: Oxford, (1959).

(19) Colton, C. K. Analysis of membrane processes for blood purification. *Blood Purif.* (1987) *5*, 202-251.

(20) Press, W. H.; Flannery, B. P.; Teukolsky, S. A.; Vetterling, W. T. *Numerical Recipes in C.* Cambridge University Press: Cambridge, (1988).

(21) Hersh, L.; Friedman, B.; Medero, R. *Method for Oscillometric Blood Pressure Determination Employing Curve Fitting.* U.S. Patent Number 5704362, (1998).

(22) Saltzman, W. M.; Radomsky, M. L. Drugs released from polymers: diffusion and elimination in brain tissue. *Chem. Eng. Sci*. (1991) *46(10)*, 2429-2444.

(23) Barry, B. W.; Brace, A. R. Permeation of oestrone, oestradiol, oestriol and dexamethasone across cellulose acetate membrane. *J. Pharm. Pharmacol*. *(*1977) *29(7)*, 397-400.

(24) Sharkawy, A. A.; Klitzman, B.; Truskey, G. A.; Reichert, W. M. Engineering the tissue which encapsulates subcutaneous implants. I. Diffusional properties. *J. Biomed. Mater. Res.* (1997) *37*, 401-412.

(25) Kim, T-K.; Burgess, D. J. Pharmacokinetics characterization of ^{14}C-vascular endothelial growth factor controlled release microspheres using rat model. *J. Pharm. Pharmacol.* (2002) *54*, 897-905.

(26) Reinhard, C. S.; Radomsky, M. L.; Saltzman, W. M.; Hilton, J.; Brem, H. Polymeric controlled release of dexamethasone in normal rat brain. *J. Controlled Release*. (1991) *16*, 331-340.

(27) Xin, Q.; Wightman, M.R. Tramsport of choline in rat brain slices. *Brain Res.* (1997) *776*, 126-132.

(28) Thorne, R.G.; Hrabetova, S.; Nicholson, C. Diffusion of epidermal growth factor in rat brain extracellular space measured by integrative optical imaging. *J. Neurophysiol*. (2004) *92*, 3471-3481.

(29) Zhou, X.; Pogue, B.W.; Chen, B.; Hasan, T. Analysis of Effective Molecular Diffusion Rates for Verteporfin in subcutaneous versus orthotopic Dunning prostate tumors. *Photochem. Photobiol.* (2004) *79(4)*, 323-331.

(30) Lankelma, J.; Luque, R.F.; Dekker, H.; Schinkel, W.; Pinedo, H.M. A mathematical model of drug transport in human breast cancer. *Microvasc. Res.* (2000) *59*, 149-161.

(31) Crank, J. *The Mathematics of Diffusion. Second Edition*. Clarendon Press: Oxford, (1975).

(32) Deen, W.M. *Analysis of Transport Phenomena*. Oxford University Press: New York, (1998).

(33) Nicholson, C. Diffusion from an injected volume of a substance in the brain tissue with arbitrary volume fraction and tortuosity. *Brain. Res.* (1985) 333, 325-329.

(34) Moussy, Y.; Hersh, L.; Dungel, P. Distribution of [^{3}H]dexamethasone in rat subcutaneous tissue after delivery from osmotic pumps. *Biotechnol. Prog.* (2006) *22(3),* 819-824.